Water Management
Volume 167 Issue WM7

Water resource assessment along the Blue Nile River, north Africa with a one-dimensional model
Ali, Crosato, Mohamed, Wright and Roelvink

ice | proceedings

Proceedings of the Institution of Civil Engineers
Water Management 167 July 2014 Issue WM7
Pages 394–413 http://dx.doi.org/10.1680/wama.13.00020
Paper 1300020
Received 02/02/2013 Accepted 30/10/2013
Published online 22/01/2014
Keywords: hydrology & water resource/mathematical modelling/water supply

ice
Institution of Civil Engineers
publishing

Water resource assessment along the Blue Nile River, north Africa with a one-dimensional model

1 Yasir S. A. Ali
PhD student, UNESCO-IHE, Delft, the Netherlands; Researcher, Hydraulics Research Center, Ministry of Water Resources and Electricity, Wad Medani, Sudan

2 Alessandra Crosato
Senior Lecturer and Researcher, UNESCO-IHE, Delft, the Netherlands; Associate Professor, Faculty of Civil Engineering and Geosciences, Delft University of Technology, Delft, the Netherlands

3 Yasir A. Mohamed
Associate Professor, UNESCO-IHE, Delft, the Netherlands; Professor, Hydraulics Research Center, Ministry of Water Resources and Electricity, Wad Medani, Sudan; Associate Professor, Faculty of Civil Engineering and Geosciences, Delft University of Technology, Delft, the Netherlands

4 Nigel G. Wright
Professor, School of Civil Engineering, University of Leeds, Leeds, UK

5 J. A. Roelvink
Professor, UNESCO-IHE, Delft, the Netherlands; Senior specialist coastal morphology, Principal investigator morphology, Deltares, Rotterdamseweg, Delft, the Netherlands


1


2

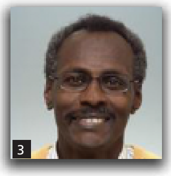
3


4


5

The water resource of the Blue Nile River in north Africa is under increasing pressure due to rapid population growth and economic development. The situation is aggravated by a lack of coordinated management and governance, partly caused by incomplete knowledge of the water supplies, uses and needs. Proper water management is particularly important now, considering the recently completed and planned mega dams on the Blue Nile River network. This paper reports on the construction of a one-dimensional hydrodynamic model covering the entire Blue Nile River system, from Lake Tana to the confluence with the White Nile, with the aim of quantifying water availability throughout the year, for different conditions. The work included an extensive field measurement campaign along the Blue River and its tributaries, both in Ethiopia and Sudan. Calibrated and validated with independent datasets, the model was used to quantify water uses in the period 2008–2010, which were then compared with the official figures. The results show that the dry season is characterised by extra water losses that should be taken into account when quantifying water needs, especially during the filling up phase of new reservoirs.

Notation

A	wet cross-sectional surface
C	Chézy coefficient
c	celerity of flood wave
Fr	Froude Number
$\mathbf{g}$	acceleration due to gravity
h	water depth
k_s	Manning–Strickler coefficient
Q	discharge
R	hydraulic radius
t	time
u	average flow velocity
$u*$	shear velocity
w_s	sediment fall velocity
x	longitudinal distance
x_i	simulated value
y_i	actual value
α	Boussinesq coefficient

1. Introduction

Water resource management is becoming increasingly difficult due to the conflicting demands from various stakeholder groups, population growth, rapid urbanisation and increasing incidences of natural disasters, especially in arid areas (Kim and Kaluarachchi, 2008). In the Blue Nile River basin, upstream runoff variability is an acute issue for the downstream countries of Sudan and Egypt as they are heavily dependent on the Nile waters. Cooperative management of the Nile waters has become urgent, considering increasing demands and climate variations (Conway, 2005; Conway and Hulme, 1996; Yates and Strzepek, 1998a, 1998b). Moreover, there are new plans for massive water resource developments for hydropower generation in Ethiopia (four large dams on the Blue Nile), as reported by BCEOM *et al.* (1998) and Hassaballah *et al.* (2011). The Grand Ethiopian Renaissance dam is currently under construction 30 km upstream of the border with Sudan (The Dam Speech, 2011) and, 150 km downstream, heightening of Roseires dam was completed in 2013. Setit and Bardana dams are under construction across the Atbara River (a Nile tributary) in Sudan.

As a result, the Nile basin countries are currently negotiating to find a common agreement on how to share the Nile waters (Nile Basin Initiative, 2003, 2004). At the time of writing (2013), six countries (Ethiopia, Tanzania, Kenya, Rwanda, Uganda and Burundi) had signed the so-called cooperative framework agreement (CFA), while Sudan, Egypt, Democratic Republic of Congo and South Sudan had not yet signed (BBC, 2010). A tripartite technical committee was formed by the three eastern Nile countries (Ethiopia, Sudan and Egypt) in early 2012 to assess the downstream impacts of the Grand Ethiopian Renaissance dam. In this context, knowledge of water uses along the Nile River is of basic importance, especially considering that the filling of the vast Grand Ethiopian Renaissance reservoir will occur in the near future. It is also important to consider that water needs vary with season, but a clear quantitative picture of these variations is still lacking. The Blue Nile accounts for 60–65% of the entire main Nile flow, with a clear bimodal seasonal pattern (Sutcliffe and Parks, 1999; UNESCO, 2004; Waterbury, 1979; Yates and Strzepek, 1998b). Therefore, every development on this river may affect the main Nile runoff in a considerable way.

The objective of this research was a description of the water distribution along the entire Blue Nile River system to quantify the availability of the water resource at all seasons and flow conditions. Hydrodynamic models, supported by field measurements, are often the most appropriate tool for this type of study. For this, a one-dimensional (1D) model of the entire Blue Nile River network was developed, including all known water uses as well as all major hydraulic structures and their operation rules. A large part of the input data was provided by the Ministry of Water Resources and Electricity of the Sudan (previously Ministry of Irrigation and Water Resources) and by the Ministry of Water Resources of Ethiopia. To fill in the most important knowledge gaps, this research included extensive fieldwork to measure river cross-sections, river bed sediment, suspended solids and flow velocity at several locations along the Blue Nile River and its main tributaries in Ethiopia and Sudan. The model was calibrated and validated on both water levels and discharges measured at selected gauging stations. The results of the model were found to describe the measured data quite well. Based on this, it is fair to state that this complete hydrodynamic model will provide reliable quantifications of the Blue Nile water availability. In particular, the model will be a useful tool to help plan the filling operations of the planned reservoirs, taking into account all downstream water needs and considering their seasonal variations as well as the seasonal variations of the water resource. The figures provided by the model will help to increase quantitative awareness, which is the first step to improve transboundary coordination in the management of the Nile water resource.

2. Study area

2.1 General characteristics of the Blue Nile basin

The basin of the Blue Nile River is shown in Figure 1. The river starts in Ethiopia as Little (Gilgile) Abbay, the largest tributary of Lake Tana, at an elevation of 2900 m above sea level (asl) (Abtew *et al.*, 2008; Easton *et al.*, 2010; Hurst, 1950) and ends in Khartoum, Sudan, where it joins the White Nile after having travelled for about 1600 km (Shahin, 1985). The Blue Nile River has a total drainage area of approximately 330 000 km^2 (Mohamed *et al.*, 2005; Johnson and Curtis, 1994) and contributes 60–65% of the total flow of the Nile River. The river basin is characterised by considerable variations in altitude, ranging from 360 m in Khartoum to 4250 m asl in the Ethiopian highlands (Betrie *et al.*, 2011). Two main landscape units can be observed – a mountainous relief that extends in Ethiopia and a flat piedmont area starting near the border with Sudan and extending out across its Sudanese portion, as shown in Figure 1.

From Lake Tana, the river travels 35 km to the Tissisat Falls, where it drops by 50 m. The river then crosses the Ethiopian highlands for about 900 km through a gorge, which is up to 1200 m deep. The river bed slope is about 1·5 m/km in Ethiopia, reducing to 0·15 m/km in Sudan. The longitudinal profile of the river is shown in Figure 2. The major tributaries of the Blue Nile are listed in Table 1, together with the surface area of their basins.

The Blue Nile crosses two different climatic zones (Table 2) – the humid Ethiopian highland zone, characterised by high rainfall and low temperatures in the wet season (July–September), and the semi-arid south-east Sudan, represented by low rainfall and high temperatures (Shahin, 1985; Sutcliffe and Parks, 1999).

During the flood season, the river and its main tributaries carry considerable amounts of suspended sediment, contributing 72–90% of the total sediment yield of the main Nile (Gaudie, 2005; Williams and Talbot, 2009). Maximum suspended sediment loads generally occur in the second half of July, a month earlier than the peak discharge (Hamid, 2001).

2.2 Hydraulic structures

From its source to the confluence with the White Nile, the Blue Nile system encounters several major structures. The first is Chara weir, built in 1998 at the outlet of Lake Tana to regulate the flow for hydropower production. The construction of the weir resulted in a change in the water flow from the lake, which counts for 7% of the total flow of the Blue Nile at the Ethiopia–Sudan border (Awulachew *et al.*, 2009; McCartney *et al.*, 2009).

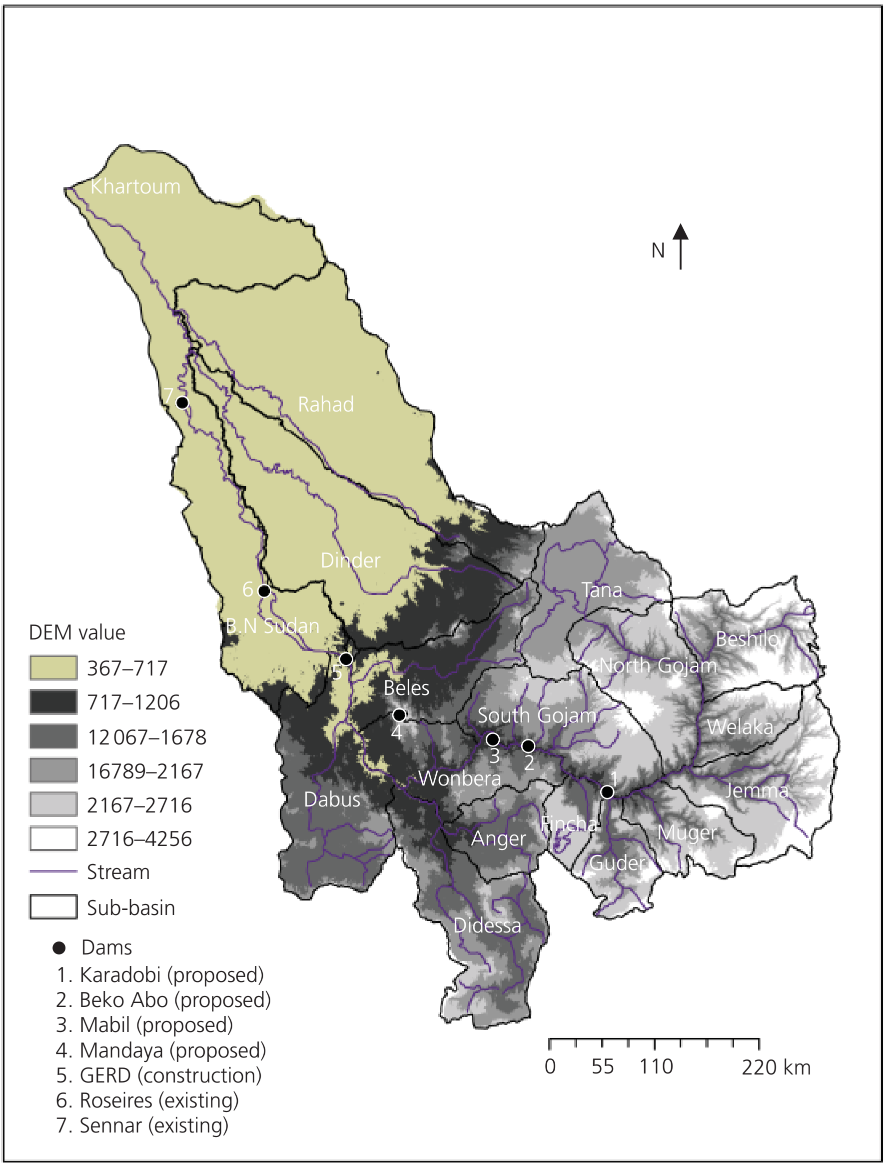

Figure 1. Blue Nile River basin topography and sub-basins. GERD, Grand Ethiopian Renaissance Dam

The second structure affecting water flow of the Blue Nile River is the Fincha dam, built in 1972 across the Fincha River, a major tributary of the Blue Nile, with a reservoir capacity of 400 million m^3 (Awulachew *et al.*, 2008) to regulate the river flow for hydropower production and sugarcane irrigation (8145 ha).

A large dam called the Grand Renaissance (Millennium) dam (Figure 1) is currently under construction in Ethiopia, 30 km upstream of the Ethiopian–Sudanese border. When completed, this will be the largest hydroelectric power plant in Africa, with a reservoir storage capacity of 74 billion m^3 (The Dam Speech, 2011).

Roseires dam, built in 1966 for irrigation and hydropower generation, is currently the first multi-purpose dam encountered by the Blue Nile. It is located 110 km downstream of the Ethiopia–Sudan border (Figure 1). The design capacity of the reservoir was 3 billion m^3 at its initial maximum impoundment level. However, being the first trap for sediments transported by the Blue Nile River, it lost a storage volume of approximately 1 billion m^3 due to sedimentation in less than 50 years (Abd Alla and Elnoor, 2007). The dam has been recently heightened by 10 m, resulting in a new reservoir capacity of 5·7 billion m^3.

Further downstream, the Blue Nile is crossed by the Sennar dam (Figure 1), built in the early 1920s 350 km south of Khartoum for irrigation and hydropower generation. The initial design reservoir capacity was 930 million m^3 but, due to siltation, the

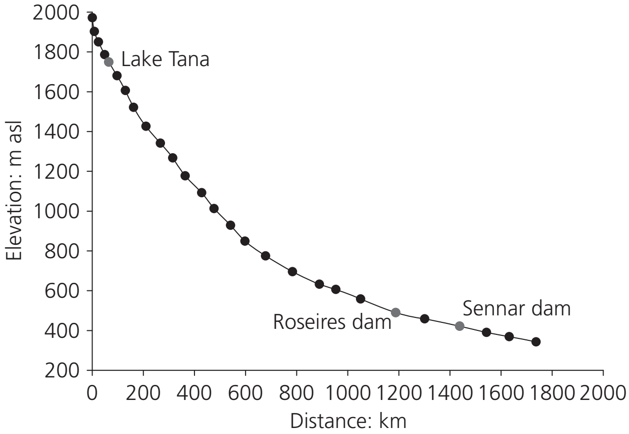

Figure 2. Blue Nile River longitudinal profile

Sub-basin	Area: km^2	Major rivers
Tana	15142	Ribb, Gumera, Megech
Beshilo	13362	Beshilo
Beles	14146	Main Beles, Gilgel Beles
North Gojam	14389	Andassa, Mened, Muga, Shina
Dabus	21252	Dabus, Hoha, Haffa
South Gojam	16762	Jedeb, Birr, Chamoga, Temcha
Jemma	15782	Robi Gumero, Jemma, Winchit
Welaka	6415	Jogola, Mechela, Selgi
Wonbera	12957	Belzmate
Fincha	4089	Neshi, Fincha
Anger	7901	Little Anger, Anger
Muger	8188	Aletu, Muger
Didessa	20087	Dabana, Didessa
Guder	7011	Debis, Guder
Dinder	37611	Dinder
Rahad	42303	Rahad
B.N Sudan	52999	Blue Nile

Table 1. Main drainage basins and major rivers of the Blue Nile basin (Archydro and SWAT)

storage capacity is now reduced to one-third of the initial volume.

Over the period 1960–1964, the United States Bureau of Reclamation carried out a major study of the land and water resources of the Blue Nile River basin in Ethiopia (US BoR, 1964). The study identified four major hydropower development sites on the Blue Nile: the border between Ethiopia and Sudan, Karadobi, Mabil and Mandaya (Figure 1). The Eastern Nile Technical and Regional Office (ENTRO) carried out pre-feasibility studies for these dams, which resulted in changed storage capacities for the Mandaya dam and Border dam (Millennium dam, under construction) and the cancellation of the Mabil dam. These studies also identified potential for hydropower generation at Beko Abo. The general characteristics of these projects are presented in Table 3.

2.3 Irrigation schemes

In Sudan, several agricultural schemes are irrigated using the waters of the Blue Nile River (Figure 3). The largest is the Gezira–Managil scheme (operating since 1925), totalling about 880 000 ha, followed by the Rahad (since 1979) and the Suki (since 1971) schemes, covering 126 000 and 37 000 ha, respectively. Finally, the North West Sennar sugar scheme (operating since 1974) and the Genaid sugar scheme (1961) cover 20 000 and 15 960 ha, respectively. The annual variations of the total volume of abstracted water for these irrigation schemes are given in Table 4, where they are compared with the annual flow of the river.

Additionally, many small irrigation schemes supplied by the pumping of water directly from the river are found along the river banks. The extraction period and the amount of water are clearly indicated in the water rights issued. Their extraction volumes, however, are unknown.

3. Data analysis and model development

3.1 Data analysis

This study relied on historical measurements of water levels and flow discharges at a series of gauging stations located along the Blue Nile River. The stations were selected based on two main criteria – their location (ensuring a good coverage of information

	Ethiopia	Source	Sudan	Source
Average rainfall: mm/year	1400–1800	Bewket and Conway, 2007 Johnson and Curtis, 1994	200–1000	Block and Rajagopalan, 2007 Gamachu, 1977
Mean annual temperature: °C	6–28	Conway, 1997	19–39	Elagib and Mansell, 2000 Hydrosult *et al.*, 2007
Mean annual evaporation: mm/year	1150	Shahin, 1985 Sutcliffe and Parks, 1999	2500	Shahin, 1985 Sutcliffe and Parks, 1999
Average annual flow Blue Nile: km^3	4–48	Sutcliffe and Parks, 1999	48–47·6	Billi and el Badri Ali, 2010

Table 2. Hydrological characterisation of the Blue Nile basin

	Border	Mandaya	Mabil	Karadobi	Beko Abo
Dam height: m	84·5	164	171	250	282
Full supply level: m asl	575	741	906	1146	1062
Capacity: million m^3	11074	15930	13600	40200	31700
Design power: MW	1400	1620	1200	1600	1940

Table 3. Characteristics of proposed hydropower projects on the Blue Nile River (US BoR and ENTRO) (Hassaballah *et al.*, 2011)

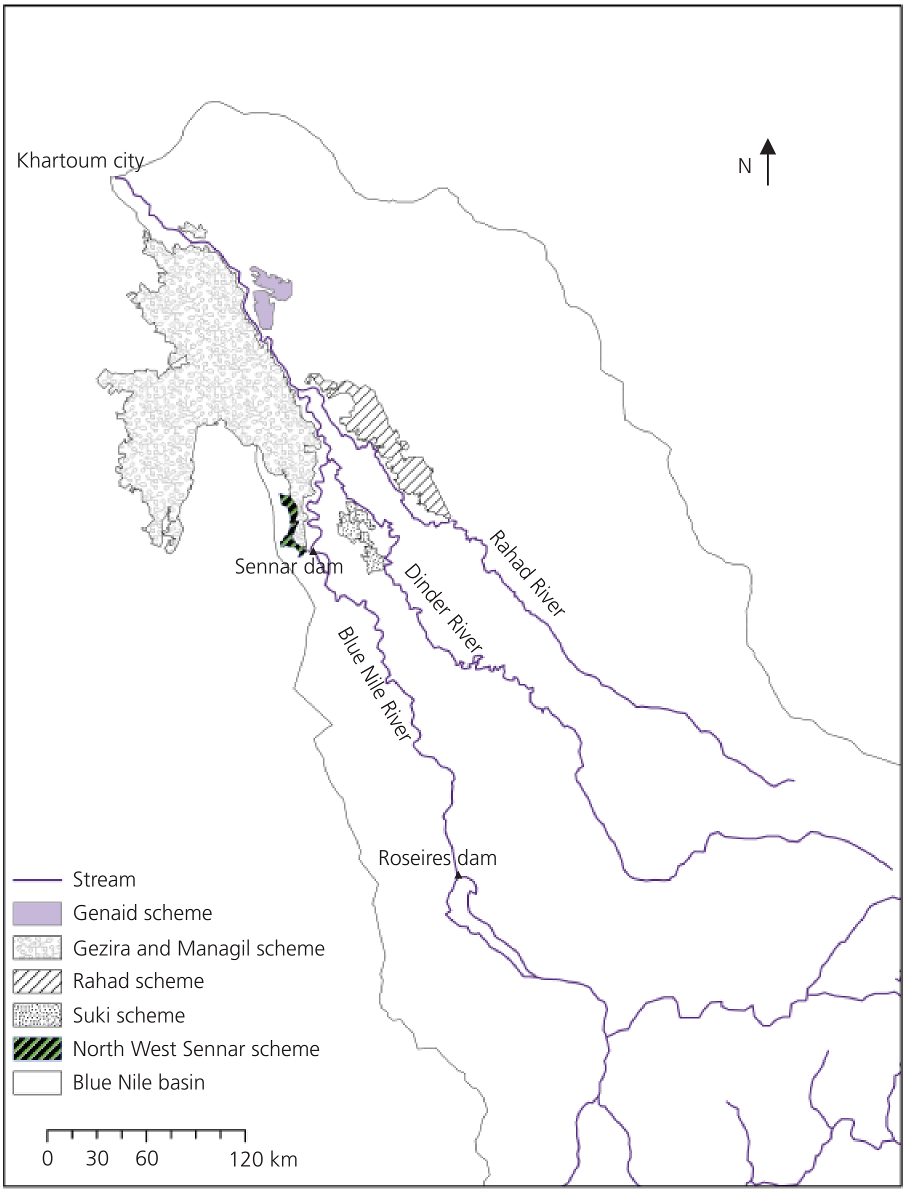

Figure 3. Locations of agricultural schemes irrigated using Blue Nile River waters

Year	Total volume of water withdrawal: million m^3	River annual flow: million m^3	Water withdrawal: %
1990	9·68	38	25·5
1991	9·786	45·4	21·6
1992	8·753	44·2	19·8
1993	10·174	56·1	18·1
1994	9·703	52·5	18·5
1995	9·471	37·1	25·5
1996	10·454	56·1	18·6
2008	9·532	59·7	16·0
2009	10·04	40·6	24·7
2010	9·922	57·3	17·3

Table 4. Volume of water withdrawal for irrigation schemes along the Blue Nile River and annual river flow

along the river course) and the availability of flow and water level records. The screening of historical data revealed a number of typing mistakes. These were corrected and flagged in Excel data files. Missing discharge data for the major tributaries were filled in with a regression equation between neighbouring stations.

A bathymetric survey of 1991 executed by the Ministry of Irrigation and Water Resources and Delft-Hydraulics includes 84 cross-sections with spacings of 5–7 km, covering the reach from Roseires dam to Khartoum, about 600 km long (Delft-Hydraulics, 1992). Other cross-sections were measured more recently at scattered locations, such as Singa just upstream of Sennar reservoir (Babiker and Salih, 2006), Suki (Babiker and Bushara, 2007), Wad Medani (Babiker *et al.*, 2010), Khartoum (HRS, 2008) and inside Roseires reservoir in different years (Abd Alla and Elnoor, 2007; Gismalla, 1993). Different references were used for the topographic data (Tiesler, 2009) for both the vertical and horizontal coordinates. This study used the UTM (Universal Transverse Mercator) WGS-84 coordinate system in the horizontal direction for the positions of the cross-sections and the Alexandria vertical datum (3 m above the local datum) for the vertical levels.

Difficulty of access to the river is the major reason for the lack of field data in Ethiopia, especially in the Blue Nile River gorge. To fill in this important knowledge gap, an extensive field survey was conducted as a part of this study in 2009. Flow velocity and bed topography were measured at 26 cross-sections along the Blue Nile River and its major tributaries using a current meter and an ecosounder in Ethiopia and an acoustic Doppler current profiler (ADCP) in Sudan. Figure 4 shows the locations of the cross-sections that were surveyed in 2009, listed in Table 5. As an example, the river cross-sections just downstream of Lake Tana (upstream boundary), at the Ethiopian–Sudanese border (middle) and at Khartoum (downstream boundary) are depicted in Figure 5 together with an image of the river at each location.

Several samples of bed sediment were collected by the Ministry of Water Resources and Electricity of Sudan and in the framework of this study by means of a grab sampler, at several locations in 2009. The samples revealed that from Lake Tana to the border between Sudan and Ethiopia the river bed is mainly sand, accounting for 80% of the material. Inside Roseires reservoir, the sand content decreases to 50%, where the river bed is composed of a mixture of silt and sand. Silt accounts for 60% of the bed material at Khartoum (Figure 6).

High sediment concentrations have been observed to damp out dunes in river channels at low Froude numbers (Best, 2005; Smith and McLean, 1977). Predicting the occurrence of bedforms is important, because the flow resistance of the river channel is determined by sediment size and form drag. This means that dune formation influences the stage–discharge relationship and this should be included in hydrodynamic models. River dunes are found in nearly all river systems with the river bed consisting of sand, small gravel or mixtures (Julien *et al.*, 2002; Paarlberg *et al.*, 2007, 2010; Wilbers and Ten Brinke, 2003).

The measured average monthly sediment concentrations (Figure 7) combined with hydrodynamic information allowed computation of the suspension number (SN). This is a parameter that characterises the level of suspension of channel bed material and is defined as

1. $$\mathrm{SN} = u* / w_\mathrm{s}$$

where $u*$ is the shear velocity (m/s) and w_s is the sediment fall velocity (m/s). This parameter can be used to infer the presence of dunes on the channel bed, since dunes seem to form for SNs smaller than 2·5 if the Froude number is smaller than 0·32 (Naqshband *et al.*, 2012).

3.2 Model development

The flow in the river network was modelled using the Sobek Rural package (www.deltares.nl). This is a 1D open-channel dynamic numerical modelling system for water flow in open channels, which has been successfully applied on river systems all over the world (Becker *et al.*, 2012; Kemink *et al.*, 2003; Prinsen and Becker, 2011; Wang *et al.*, 2007). The model is based on the Saint-Venant equations for unsteady flow. The continuity equation is

2. $$\frac{\partial A}{\partial t} + \frac{\partial Q}{\partial x} = 0$$

and the momentum equation is

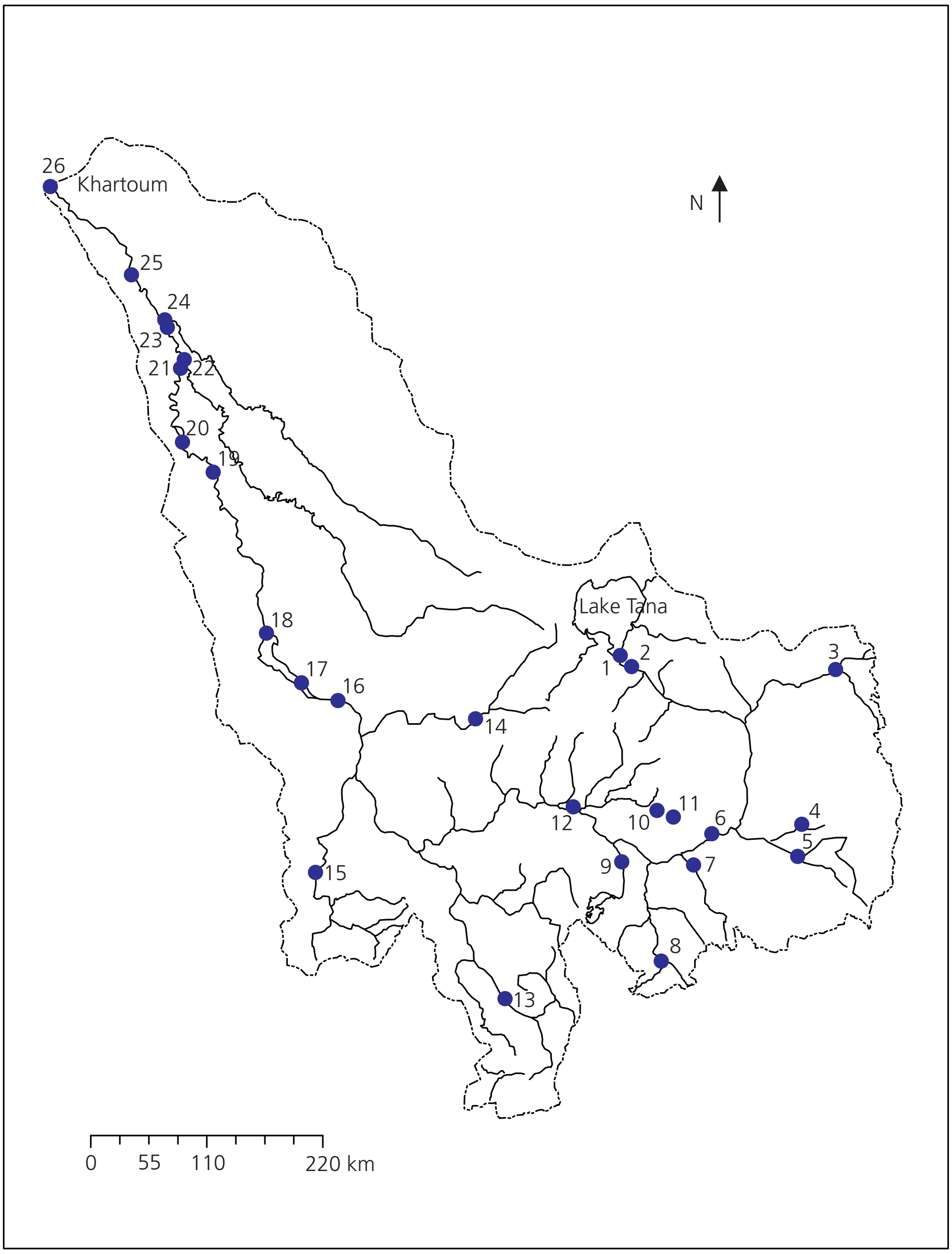

Figure 4. Locations of the measured cross-sections (see Table 3)

$$\frac{\partial Q}{\partial t} + \frac{\partial}{\partial x}\left(\alpha \frac{Q^2}{A}\right) + \boldsymbol{g}A\frac{\partial h}{\partial x} + \frac{\boldsymbol{g}Q|Q|}{C^2RA} = 0 \tag{3}$$

in which A is the wet cross-sectional surface (m^2), Q is the discharge (m^3/s), t is time (s), x is the longitudinal distance (m), α is the Boussinesq coefficient, $\boldsymbol{g}$ is acceleration due to gravity (m/s^2), h is the water depth (m), C is the Chézy coefficient (m$^{1/2}$/s) and R is the hydraulic radius (m).

Computation of the water levels and discharges in the Sobek-flow-network was performed with the Delft-scheme. This scheme solves the Saint-Venant continuity and momentum equations by means of a staggered grid in which the water levels are defined at the connection nodes and calculation points, while the discharges are defined at the intermediate reaches or reach segments. The software allows for the inclusion of several types of hydraulic structures such as weirs, sluice gates, pumps and locks, as well as their operation rules.

The domain of the developed model covers the Blue Nile River from the outlet of Lake Tana (upstream boundary) to Khartoum (downstream boundary). The length of the main stream of the river is about 1600 km – about 950 km in Ethiopia and 650 km

1	Downstream Lake Tana	14	Beles River
2	Andassa River	15	Dabus River
3	Beshilo River	16	Abbay River at Border
4	Walaka River	17	Blue Nile River at Roseires 1
5	Jemma River	18	Blue Nile River at Roseires 2
6	Abbay River at Kessie	19	Blue Nile River at Singa
7	Muger River	20	Blue Nile River at Kassab
8	Guder River	21	Dinder River
9	Fincha River	22	Blue Nile River at Nor Al Deen
10	Chemoga River	23	Blue Nile River at Wad Medani
11	Yeda River	24	Rahad River
12	Abbay River at Bure	25	Blue Nile River at Hilalia
13	Didessa River	26	Blue Nile River at Khartoum

Table 5. Denomination of measuring stations shown in Figure 4

in Sudan. A large part of the cross-sectional data from the Sudanese part of the river dates from 1990 but, unfortunately, the only cross-sections available for the Ethiopian part of the river are those measured in 2009 in the framework of this project. The total number of cross-sections available for the entire Blue Nile River network is 168.

To allow sufficient accuracy, the space step of the longitudinal (1D) grid was set equal to 3000 m. The value of the timestep was derived imposing the Courant condition

4. $$c\frac{\Delta t}{\Delta x} \leqslant 10$$

in which c is the celerity of the flood wave (m/s).

According to the available data, at El Deim station

- average flow width = 500 m
- maximum daily change in discharge in the rising limb = 1500 m^3/s
- water level change at maximum daily discharge change = 0·75 m
- celerity of the flood wave = 4 m/s.

Based on Equation 4, the timestep must satisfy the condition $\Delta t < 7500$ s (125 min) so, in the model, the timestep was set to 1 h.

The daily outflow discharge from Lake Tana at Bahr Dar defines the upstream boundary conditions of the hydrodynamic model, whereas the daily discharge time series from the major tributaries listed in Table 1 are lateral flows entering the system. Water extraction for the irrigation schemes are lateral flows leaving the system. The time series water levels at Khartoum station define the downstream boundary conditions.

The model includes Sennar and Roseires dams along with their operation rules. The model schematisation, including the dams and the hydrological stations is depicted in Figure 8.

3.3 Description of model calibration and validation

Model calibration and validation were carried out by comparing computed to measured water levels at El Deim, just upstream of Roseires dam (inside the reservoir), Wad Al Ais, just upstream of Sennar dam (inside the reservoir), Hag Abdalla and Wad Medani (Table 6), and by comparing computed with measured discharges at Kessie Bridge, El Deim, just downstream of Roseires dam and just downstream of Sennar dam station (Table 7).

The primary parameter required for calibration of a 1D hydrodynamic model such as Sobek Rural is bed roughness (McGahey *et al.*, 2012). The Manning–Strickler coefficient was chosen for the calibration instead of the Chézy coefficient, C. The model can freely calculate C considering the local hydraulic radius taken from the last iteration loop. The Strickler formula is one of the methods to define the bed roughness. The actual value of the Chézy coefficient is computed using

5. $$C = k_s R^{1/6}$$

in which k_s is the Manning–Strickler coefficient ($m^{1/3}/s$) and R is the hydraulic radius (m). The calibration was performed by adjusting the values of k_s in order to get a good reproduction of the observed water level and discharges at a number of gauging stations.

The river network was divided into three reaches according to the positions of Roseires and Sennar dams: reach 1 represents the river upstream of Roseires dam; reach 2 represents the river between the two dams of Roseires and Sennar; reach 3 describes the river from Sennar dam to Khartoum.

The model was calibrated for the period 1990–1993. Several runs

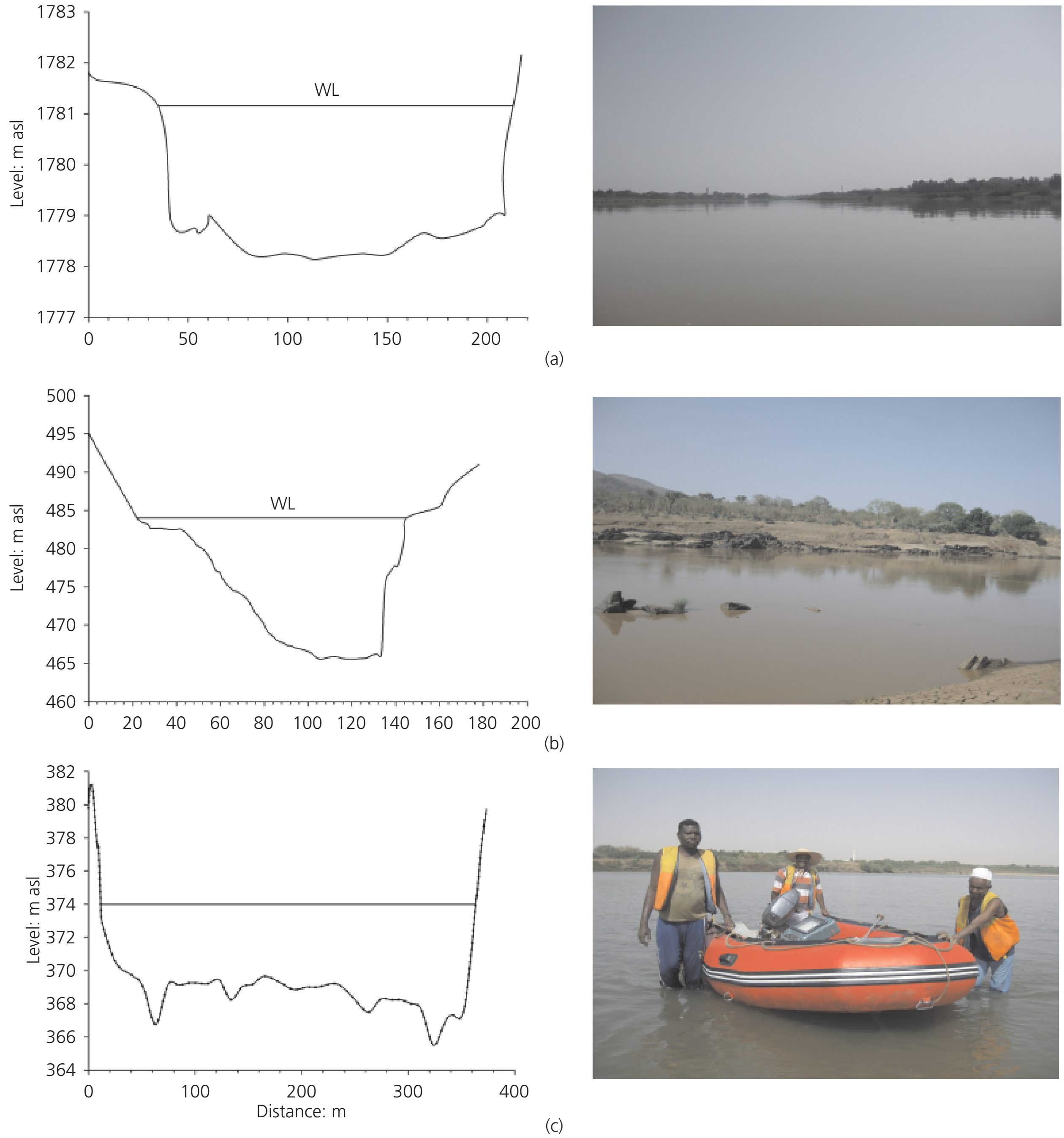

Figure 5. Blue Nile River cross-sections downstream of Lake Tana (a), at the Ethiopian–Sudanese border (b) and at Khartoum (c). Note that the graphs have different horizontal and vertical scales

were carried out with different k_s values ranging between 30 $m^{1/3}/s$ and 70 $m^{1/3}/s$ with the aim of optimising reproduction of the observed water levels and discharges at a number of gauging stations. The adjusted values of k_s were found to be 60, 55, 50 and 40 $m^{1/3}/s$ in the reach from Lake Tana to El Deim, from El Deim to Roseires dam, between Roseires dam and Sennar dam, and in the reach between Sennar dam and Khartoum, respectively.

Because the calibration process involves some adjustments of parameter values that are optimised to fit a certain dataset, good model calibration cannot automatically ensure that the model performs equally well for other periods and circumstances. Therefore, model validations on independent data are required. The model was therefore validated by comparing its results to measured data for the three years 1994, 1995 and 1996.

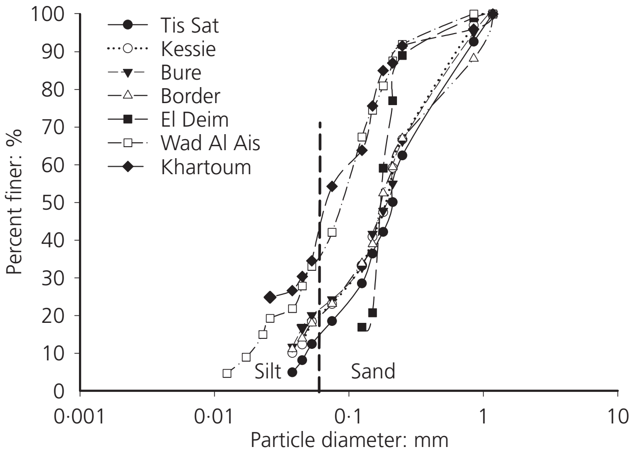

Figure 6. Composition of Blue Nile River bed material

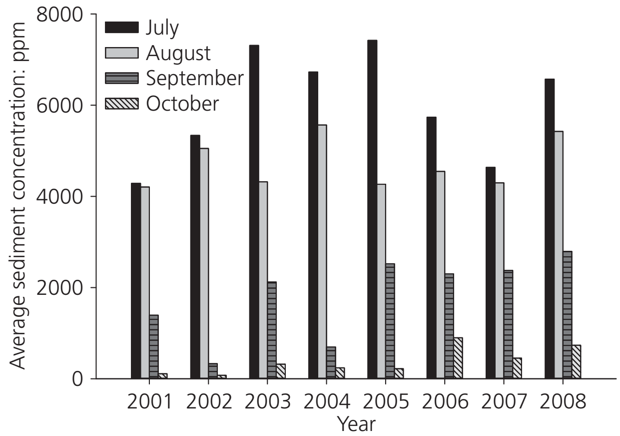

Figure 7. Average monthly sediment concentration of Blue Nile downstream of the Sennar dam

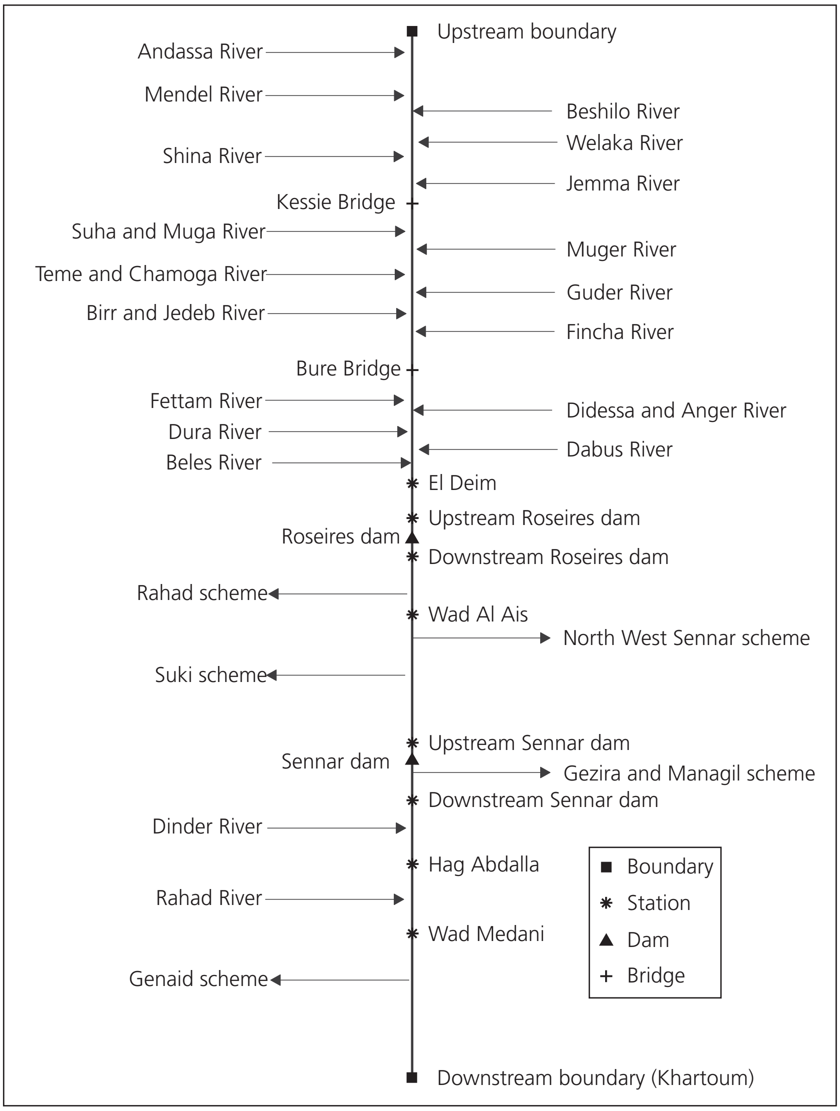

Figure 8. Model schematisation

Branch	Station name[a]	Distance upstream of Khartoum: km
Reach 1	El Deim (a)	740
	Upstream Roseires dam (b)	629
Reach 2	Wad Al Ais (c)	436·5
	Upstream Sennar dam (d)	351
Reach 3	Hag Abdalla (e)	282·5
	Wad Medani (f)	200·5

[a] The letters following station name refer to parts (a)–(f) in Figures 9, 11 and 13.

Table 6. Water level calibration and validation chaining

Branch	Station name[a]	Distance upstream Khartoum (km)
Reach 1	Kessie Bridge (a)	1340
	El Deim (b)	740
Reach 2	Downstream Roseires dam (c)	630
Reach 3	Downstream Sennar dam (d)	345

[a] The letters following station name refer to parts (a)–(d) in Figures 10, 12 and 14.

Table 7. Discharge calibration and validation chaining

There are several statistical measures that can be used to evaluate the performance of simulation models, among which are assessment of the correlation coefficient (R^2), the Nash–Sutcliffe efficiency (NSE) (Nash and Sutcliffe, 1970) and the root mean squared error (RMSE). The correlation coefficient R^2 reflects the linear relationship between observed and simulated data and is thus insensitive to either an additive or a multiplicative factor. Some authors recommend this parameter when large-scale models with gridded fields are involved. R^2 ranges from 0 to 1, with higher values indicating less error variance; typically, values greater than 0·5 are considered acceptable (Santhi and Arnold, 2001; van Liew *et al.*, 2003). R^2 is given by

$$R^2 = \frac{\sum_{i=1}^{n}(x_i - \bar{x})^2(y_i - \bar{y})^2}{\sum_{i=1}^{n}(x_i - \bar{x})^2\sum_{i=1}^{n}(y_i - \bar{y})^2} \quad (6)$$

where x_i is the simulated value and y_i is the actual value.

The NSE indicates how well a plot of observed versus simulated data fits the 1:1 line. It is computed according to

$$\text{NSE} = 1 - \frac{\sum_{i=1}^{n}(y_i - x_i)^2}{\sum_{i=1}^{n}(y_i - \bar{y})^2} \quad (7)$$

The RMSE is a commonly used error index (Chu and Shirmohammadi, 2004; Singh *et al.*, 2004; Vazquez-Amábile and Engel, 2005) and it gives the standard deviation (SD) of the model prediction error. Values close to zero indicate a perfect fit. Its value should be compared with the standard deviation of the measured data. Values less than half of the standard deviation of the measured data are considered acceptable (Singh *et al.* (2004)). The RMSE is given by

$$\text{RMSE} = \left(\frac{(x_1 - y_1)^2 + (x_2 - y_2)^2 + \cdots + (x_n - y_n)^2}{n}\right)^{1/2} \quad (8)$$

4. Results

4.1 Results of data analysis

High concentrations of suspended solids were measured during high flow conditions, ranging between 3000 mg/l and 18 222 mg/l at El Deim and between 3720 mg/l and 15 044 mg/l just downstream of Roseires dam. These concentrations results in SNs ranging between 2·8 and 3·5. Given that the corresponding

Station	Flow	Q: m^3/s	Water level: m	A: m^2	h: m	U: m/s	Fr	u^*: m/s	D_{50}: mm	w_s: m/s	SN
El Deim	Low	155	488	550	3	0·3	0·05	0·054	0·18	0·0323	1·66
	Medium	960	489	1279	4·6	0·8	0·11	0·067	0·18	0·0323	2·07
	High	6126	493	2974	8·2	2·1	0·23	0·09	0·18	0·0323	2·78
Was Al Ais	Low	300	422	758	3·2	0·4	0·07	0·018	0·09	0·0004	2·18
	Medium	944	423	1008	3·6	0·9	0·16	0·019	0·09	0·0004	2·32
	High	5842	426	2175	8·1	2·7	0·3	0·028	0·09	0·0004	3·48

Table 8. Suspension numbers at El Deim and Wad Al Ais station

Froude numbers are smaller than 0·32, it is possible to assume that, during high flows, dunes do not form in the Sudanese part of the Blue Nile. However, dunes are expected to form at lower flow stages when the SN is smaller than 2·5 (Table 8).

4.2 Model calibration and validation

The results of model calibration in terms of water levels and discharges are shown in Figures 9 and 10, respectively, for the period January 1990 to January 1994. The comparison between

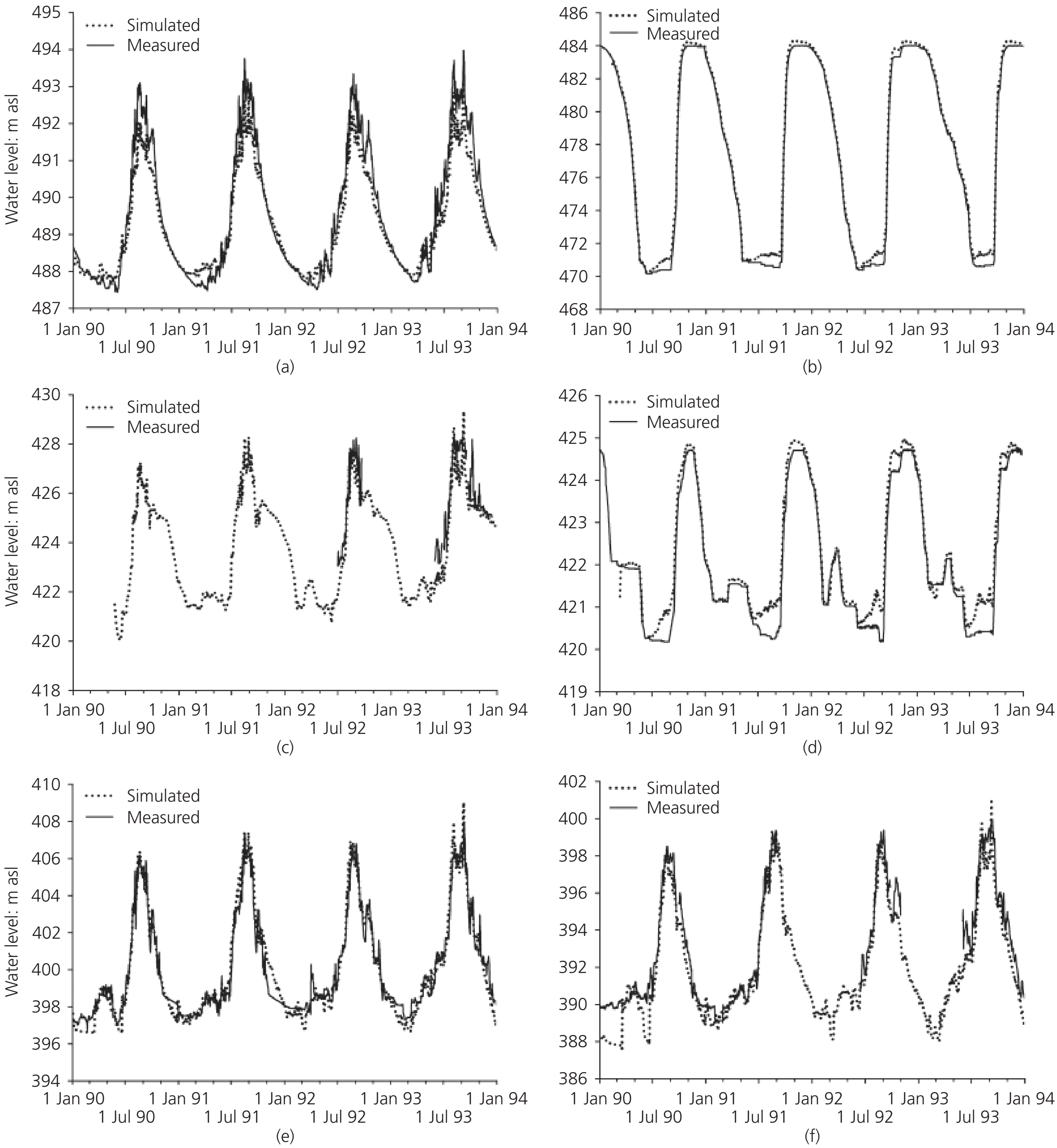

Figure 9. Comparison of observed and simulated water levels at (a) El Deim, (b) upstream of Roseires dam, (c) Wad Alais, (d) upstream of Sennar dam, (e) Hag Abdalla and (f) Medani for the period January 1990 to January 1994

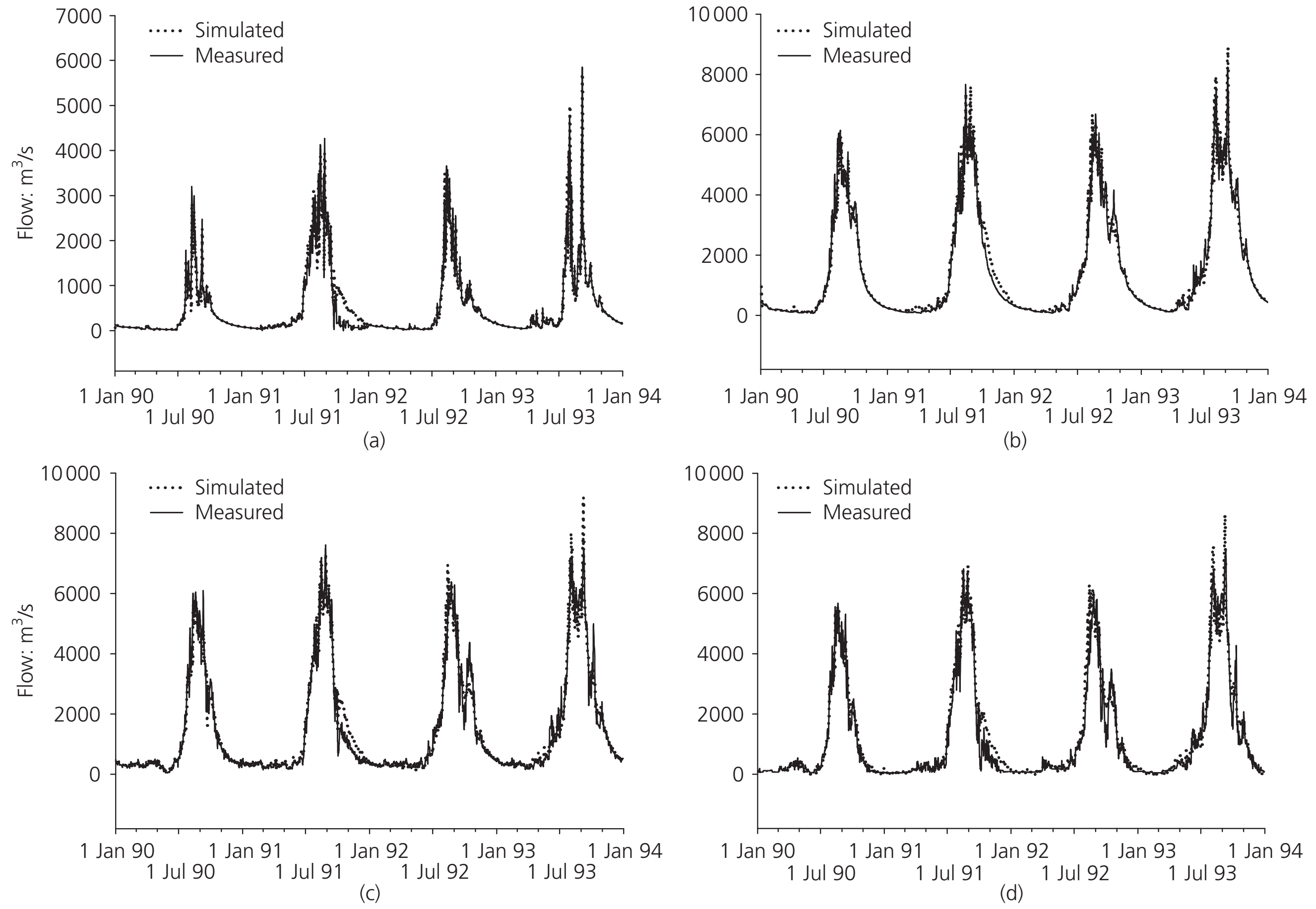

Figure 10. Comparison of observed and simulated discharges at Kessie Bridge (a) and El Deim (b) and from Roseires dam (c) and Sennar dam (d) for the period January 1990 to January 1994

computed and measured water levels shows a general tendency to slightly underestimate high-flow levels and slightly overestimate low-flow levels inside the reservoirs of Roseires and Sennar, whereas the model performs well for the other stations along the river. The comparison between modelled and measured discharges shows good agreement between the model and measurements.

The results for January 1994 to January 1997 are shown in Figures 11 and 12. Again, the model shows a slight under-prediction of peak-flow levels and a slight over-prediction of low-flow levels inside the reservoirs of Roseires and Sennar, whereas the model performs well for the other stations along the river. The model predicted discharges during low flows well, but overestimated the highest discharges at all stations (Figure 12).

The RMSE, NSE and correlation coefficients were computed to quantify the model performance. Tables 9 and 10 show the values of these indexes for simulations of water levels and discharges in the periods 1990–1993 (calibration) and 1994–1996 (validation), respectively. Model calibration resulted in correlation coefficients of 0·947–0·999 and NSE values of 0·910–0·999 for the water levels (Table 9). For the discharges (Table 10), the correlation coefficients fell to 0·950–0·972 and the NSE values to 0·044–0·970. Model validation resulted in R^2 values between 0·930 and 0·998 and NSE values of 0·926–0·995 for the water levels. For the discharges, R^2 values were 0·894–0·964 and NSE values 0·880–0·959. The results show that RMSE values were always less than 50% of the standard deviation of the measured data and model performance can therefore be considered good.

5. Assessment of water distribution

Since most data used for model setup, calibration and validation date from the 1990s, the model strictly represents the Blue Nile River behaviour 15–20 years ago. To check its performance for more recent years, the model was applied to study water levels and discharge distributions in 2008, 2009 and 2010. The results (Figures 13 and 14) show that the agreement between simulated and measured water levels and discharges is still good. Similarly to the calibration and validation runs, the model tends to over-predict low-flow water levels inside the reservoirs of Roseires and Sennar, but now also in the reach between the two dams, as well as from Sennar dam to Khartoum, and to over-predict peak

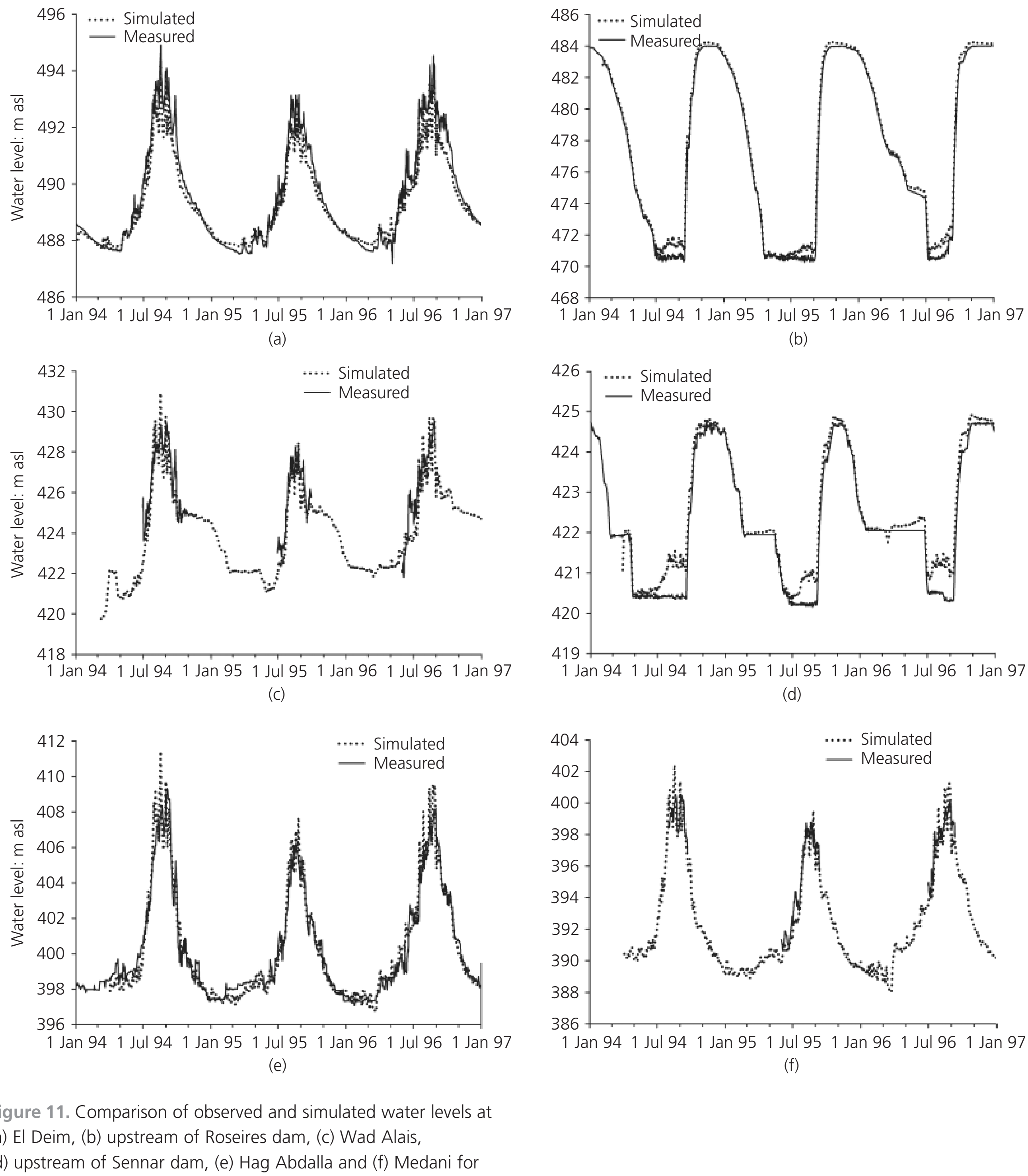

Figure 11. Comparison of observed and simulated water levels at (a) El Deim, (b) upstream of Roseires dam, (c) Wad Alais, (d) upstream of Sennar dam, (e) Hag Abdalla and (f) Medani for the period January 1994 to January 1997

discharges. This model behaviour could be an indication of unknown water uses or water losses during the dry season, but this can be established only by analysing the model performance considering its simplifications and shortcomings.

Several irrigation schemes in Sudan withdraw water from the Blue Nile River, especially in the reach between the dams of Roseires and Sennar and from Sennar to Khartoum (Section 2.3). The model includes water extractions by the irrigation schemes listed in Table 4, but does not include the additional small (private) schemes, since it is difficult to assess their amount of abstraction. For this, pumping rates and pumping hours should be

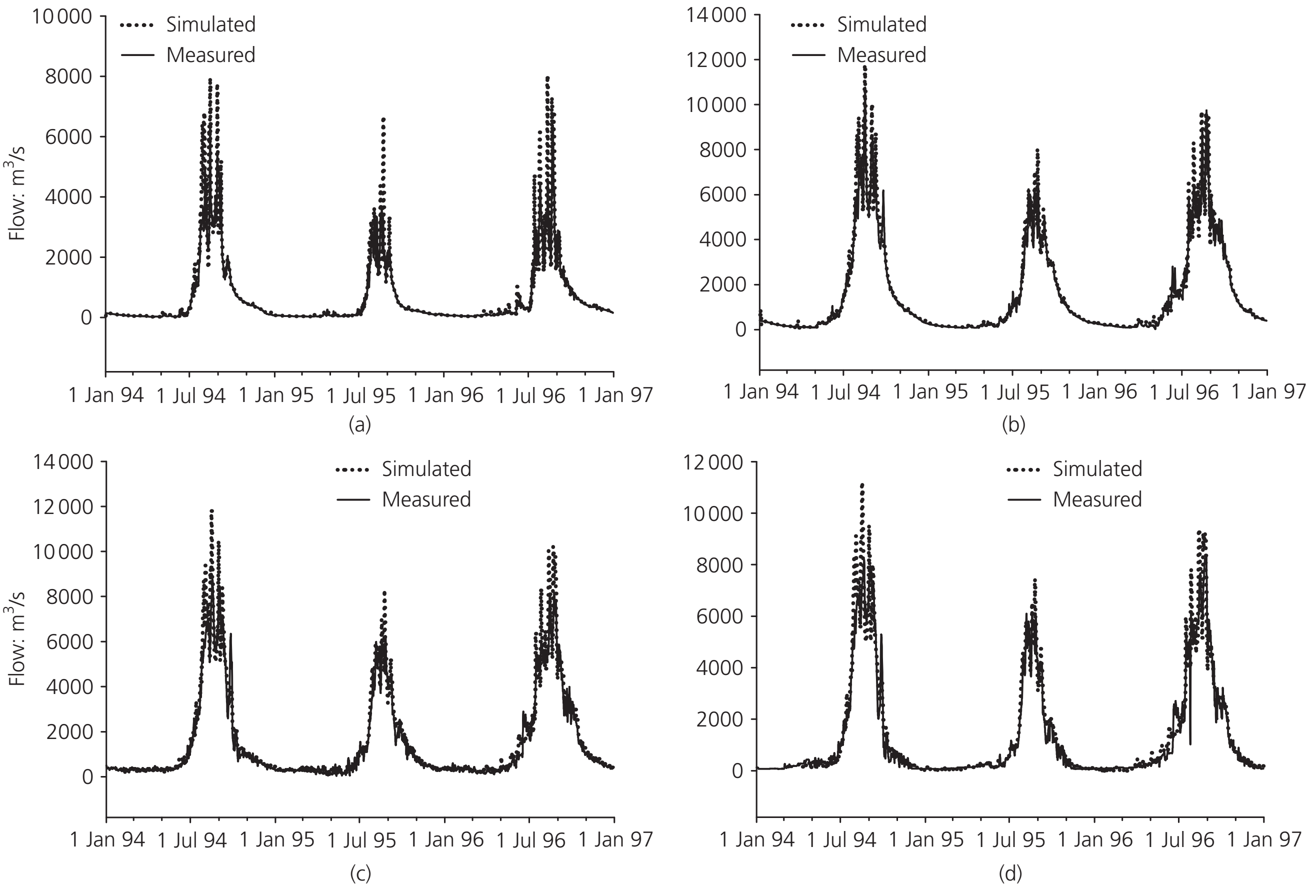

Figure 12. Comparison of observed and simulated discharges at Kessie Bridge (a) and El Deim (b) and from Roseires dam (c) and Sennar dam (d) for the period January 1994 to January 1997

	Calibration				Validation			
	R^2	NSE	RMSE	SD	R^2	NSE	RMSE	SD
El Deim	0·977	0·910	0·26	1·73	0·978	0·926	0·27	1·81
Upstream Roseires	0·999	0·995	0·2	5·55	0·998	0·995	0·22	5·36
Wad Al Ais	0·999	0·999	0·39	2·13	0·955	0·947	0·47	2·19
Upstream Sennar	0·975	0·955	0·25	1·59	0·974	0·947	0·26	1·6
Hag Abdalla	0·953	0·943	0·59	2·7	0·951	0·943	0·67	3·02
Wad Medani	0·947	0·944	0·69	3·02	0·930	0·927	0·8	3·01

Table 9. Water levels: calibration and validation correlation coefficients and RMSE

used as inputs to precisely calculate their consumption, but no-one knows these variables and there are thousands of small pumping schemes in operation.

Over-prediction of low-flow water levels could be caused by not taking into account these water extractions, but it could also be due to systematic overestimation of the channel bed roughness during low flows. In the model, roughness varies as a function of water depth without taking into account any additional flow resistance due to dune formation. For the particular case of the sand-bed Blue Nile, we can expect that dunes form at low flows but not at high flows when the concentration of suspended solids is very high (Section 3.1). This means that, most probably, the Blue Nile river bed is much rougher during low flows than during

Name	Calibration				Validation			
	R^2	NSE	RMSE	SD	R^2	NSE	RMSE	SD
Kessie Bridge	0·960	0·958	155·82	777·05	0·894	0·88	341·29	1049·17
El Deim	0·972	0·970	295·97	1783·05	0·964	0·959	385·59	2018·27
Downstream Roseires	0·959	0·958	363·92	1790·43	0·943	0·936	470·35	1965·61
Downstream Sennar	0·950	0·944	387·45	1730·54	0·934	0·932	524·08	2043·13

Table 10. Discharges: calibration and validation correlation coefficients and RMSE

high flows. The effect of using one single value of the Manning–Strickler coefficient means that channel roughness during low flows is most probably underestimated rather than overestimated by the model. Based on this, the discrepancy between measured and computed water levels during the low flow season appears to be related to losses of water that could be caused by evaporation (included in the model), groundwater recharge (not included in the model) and water withdrawal (partly included in the model) rather than to bed roughness overestimation.

It is difficult to thoroughly quantify the losses due to groundwater recharge, but it can be reasonably assumed that most of these losses are due to the water abstractions that have not been quantified. The model was finally used to quantify the total water losses in the region between Roseires and Khartoum, which include water extraction and groundwater recharge. These were found to be 2·675 billion m^3/year, on average, for the years 2008 to 2010, which is more than 25% of the known water extraction for agriculture (Table 4). The same exercise applied to the period 1990–1996 resulted in yearly averaged water losses of 1·457 billion m^3/year, about 15% of the known extracted volumes.

6. Discussion and conclusions

This paper reports on the construction of a 1D hydrodynamic model of the entire Blue Nile River system to be used to quantify the availability of the water resource throughout the year. The model was built on cross-sectional data from the 1990s for the Sudanese part of the river and from 2009 for the Ethiopian part. It was calibrated on the period 1990–1993 and validated on the period 1994–1996.

The simulations showed good correlation coefficients between computed and measured water levels and discharges for both the calibration and validation runs. The RMSE values for calibration and validation were less than 50% of the standard deviations. These results give confidence in the model, particularly considering the need to estimate discharges from measured water levels at locations where discharge measurements are scarce or absent. However, since most of the data used to set up, calibrate and validate the model were from the 1990s, the model strictly represents the behaviour of the Blue Nile River 15–20 years ago. To check its performance on recent years, the model was applied to study water levels and water distribution in 2008, 2009 and 2010. Comparison of computed and measured water levels and discharges revealed that the model also performs well for the present situation. From this, it can be concluded that morphological changes occurring over the last 20 years do not seem to have affected the hydrodynamic behaviour of the Blue Nile River system in a relevant way.

However, morphological changes can be expected due to vast ongoing deforestation of the upper catchment, which has caused an increase of sediment input to the river in its upper parts. This might have already resulted in local aggradation of the river bed and in an increase of the longitudinal slope. Most of this sediment is believed to have settled inside Roseires reservoir, in irrigation canals and to a minor extent inside Sennar reservoir, so increased sediment inputs are expected to have had only minor effects on the Sudanese part of the river. To check this and to quantify the river morphological changes, a new topographic campaign combined with morphodynamic modelling should be implemented in the future.

The cross-sections measured between the upstream boundary and the Ethiopian–Sudanese border are limited in number due to the difficulty of access to the river flowing inside a deep gorge. Discharge measurements are also scarce, especially for the upper part of the river. These factors contributed to model inaccuracy. To improve model performance, especially in the Ethiopian part, additional measuring campaigns along the Blue Nile and its tributaries are recommended in order to collect new data on cross-sectional profiles, flow velocity, bed material and suspended solids.

The Blue Nile River basin is currently subject to many challenges, such as a growing population that will increase water demand and dam construction which may affect the river regime during low flows in particular. Critical moments related to the availability of the water resource can be expected in the future during the filling phase of the newly constructed reservoirs.

Based on discrepancies between computed and measured water levels, it was possible to identify unknown water losses in unquantified uses, evaporation from Roseires and Sennar lakes

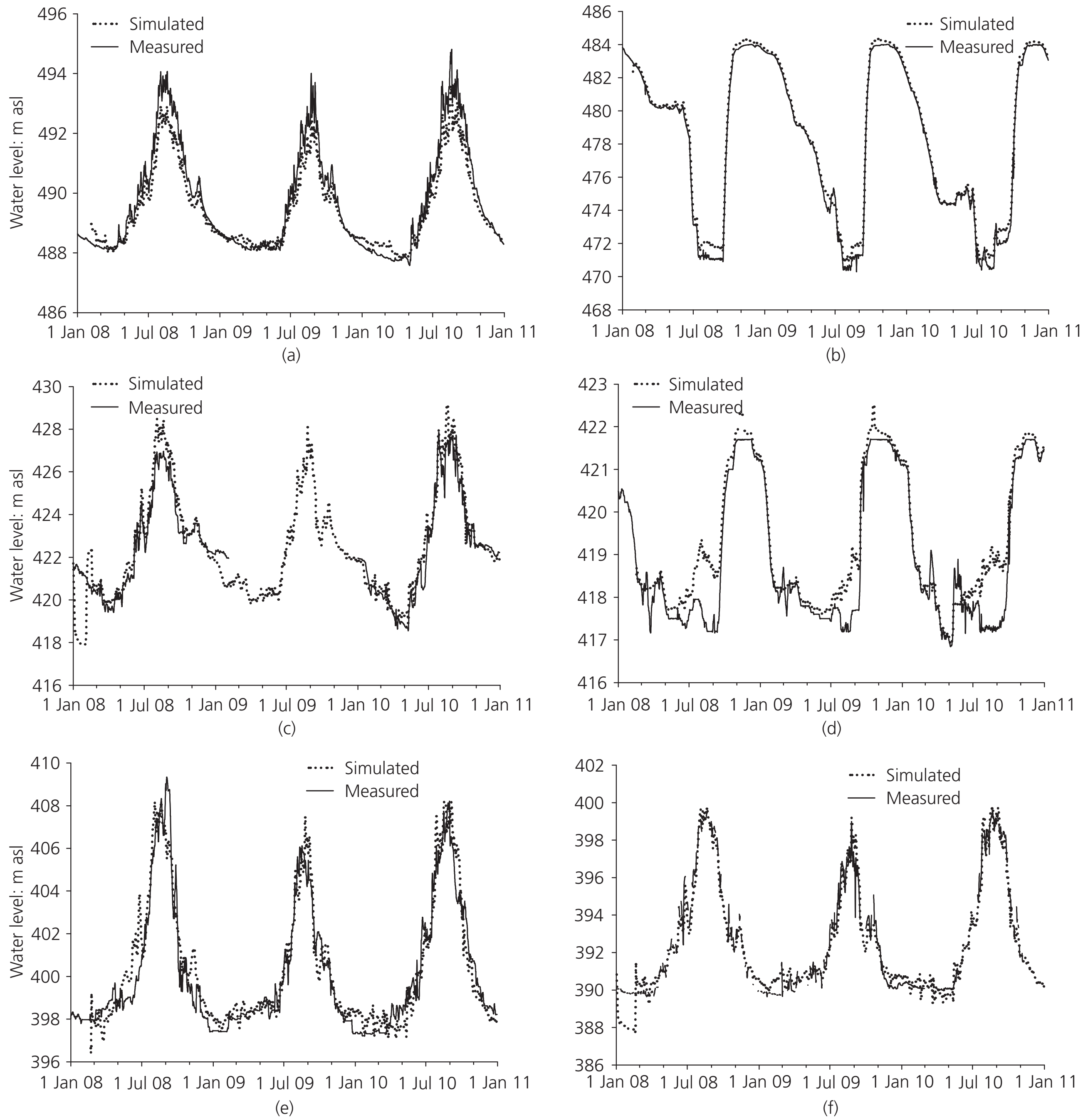

Figure 13. Comparison of observed and simulated water levels at (a) El Deim, (b) upstream of Roseires dam, (c) Wad Alais, (d) upstream of Sennar dam, (e) Hag Abdalla and (f) Medani for January 2008 to January 2011

and possibly also groundwater recharge. These water losses should be included in the overall water budgets of the basin. Thanks to its good performance, the model will be a reliable tool with which to simulate hydrodynamic conditions along the Blue Nile during and after the construction of the planned large dams in Ethiopia.

Acknowledgements

The study was conducted as part of a larger research programme called 'In search of sustainable catchments and basin-wide solidarities in the Blue Nile River Basin', funded by the Foundation for the Advancement of Tropical Research (WOTRO) of the Netherlands Organization for Scientific Research (NWO),

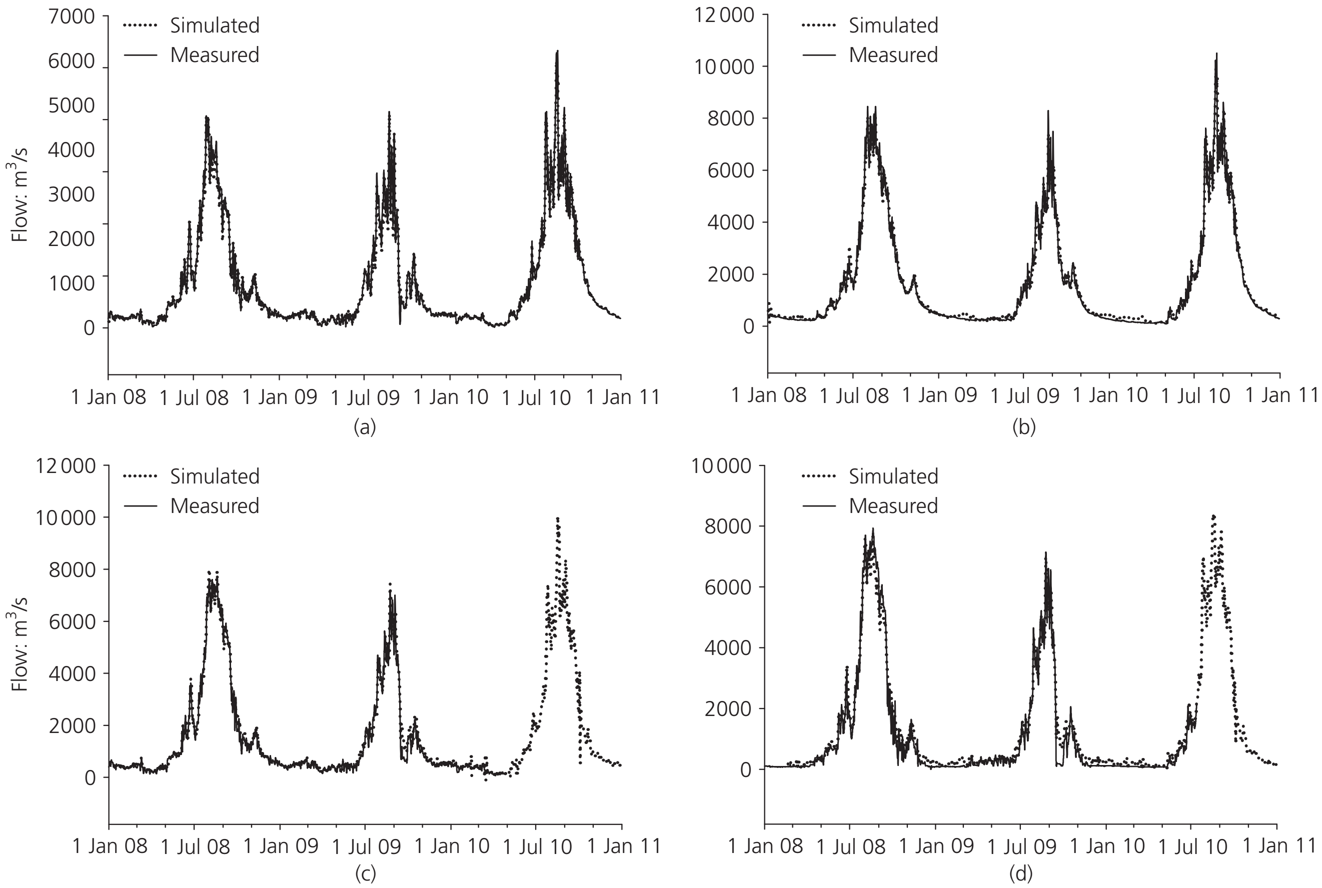

Figure 14. Comparison between observed and simulated discharges at Kessie Bridge (a) and El Deim (b) and from Roseires dam (c) and Sennar dam (d) for the period January 2008 to January 2011

UNESCO-IHE, the University of Khartoum and Addis Ababa University. The authors are grateful to the Ministry of Water Resources and Electricity, Hydraulic Research Center, Wad Madani, Sudan and the Ministry of Water Resources, Addis Ababa, Ethiopia, for providing data free of charge. The authors wish to thank Dr Kees Sloff for his helpful advice during the modelling phase and Chol Abel for his valuable contribution in revising the English text.

REFERENCES

Abd Alla MB and Elnoor K (2007) *Hydrographic Survey of Roseires Reservoir*, vol. 1. Ministry of Irrigation and Water Resources, Khartoum, Sudan.

Abtew W, Melesse AM and Dassalegne T (2008) Characteristics of monthly and annual rainfall of the Upper Blue Nile Basin. *Proceedings of Hydrology and Ecology of the Nile River Basin under Extreme Conditions Conference, Addis Ababa, Ethiopia*, pp. 250–262.

Awulachew SB, McCartney M, Steenhuis TS and Ahmed AA (2008) *A Review of Hydrology, Sediment and Water Resource Use in the Blue Nile Basin*. International Water Management Institute, Colombo, Sri Lanka.

Awulachew SB, Erkossa T, Smakhtin V and Fernando A (2009) *Improved Water and Land Management in the Ethiopian Highlands: Its Impact on Downstream Stakeholders Dependent on the Blue Nile*. International Water Management Institute, Colombo, Sri Lanka, http://dx.doi.org/10.3910/2009.201.

Babiker A and Bushara A (2007) *Investigation of Irrigation Pump Site on the Blue Nile River at Kassab*. Ministry of Irrigation and Water Resources, The Hydraulics Research Station, Wad Medani, Sudan.

Babiker A and Salih Y (2006) *Blue Nile River Bank Erosion at Singa City*. Ministry of Irrigation and Water Resources, The Hydraulics Research Station, Wad Medani, Sudan.

Babiker A, Salih Y and Osman M (2010) *Selection of Gauging Station Site on the Blue Nile River at Wad Medani City*. Ministry of Irrigation and Water Resources, The Hydraulics Research Station, Wad Medani, Sudan.

BBC (2010) *East Africa seeks more Nile water from Egypt*. See http://news.bbc.co.uk/2/hi/africa/8682387.stm (accessed 14/05/2010).

BCEOM, ISL and BRGM (1998) *Abbay River Basin Integrated Development Master Plan Project*. Report to Ministry of Water Resources, Addis Ababa, Ethiopia.

Becker BPJ, Schwanenberg D, Schruff T and Hatz M (2012) Conjunctive real time control and hydrodynamic modelling in application to Rhine River. *Proceedings of 10th Intentional Conference on Hydroinformatics, HIC 2012, Hamburg, Germany*.

Best J (2005) The fluid dynamics of river dunes: a review and some future research directions. *Journal of Geophysical Research* **110(F04S02)**: 1–21.

Betrie G, Mohamed Y, van Griensven A, Srinivasan R and Mynett A (2011) Sediment management modelling in Blue Nile Basin using SWAT model. *Hydrology and Earth System Sciences* **15(3)**: 807–818.

Bewket W and Conway D (2007) A note on the temporal and spatial variability of rainfall in the drought-prone Amhara region of Ethiopia. *International Journal of Climatology* **27(11)**: 1467–1477.

Billi P and el Badri Ali O (2010) Sediment transport of the Blue Nile at Khartoum. *Quaternary International* **226(1–2)**: 12–22.

Block P and Rajagopalan B (2007) Interannual variability and ensemble forecast of upper Blue Nile Basin kiremt season precipitation. *Journal of Hydrometeorology* **8(3)**: 327–343.

Chu TW and Shirmohammadi A (2004) Evaluation of the SWAT model's hydrology component in the piedmont physiographic region of Maryland. *Transactions of the American Society of Agricultural Engineers* **47(4)**: 1057–1073.

Conway D (1997) A water balance model of the upper Blue Nile in Ethiopia. *Hydrological Sciences Journal* **42(2)**: 265–286.

Conway D (2005) From headwater tributaries to international river: observing and adapting to climate change variability and change in Nile Basin. *Global Environmental Change* **15(2005)**: 99–114.

Conway D and Hulme M (1996) The impacts of climate variability and climate change in the Nile Basin on future water resources in Egypt. *Water Resources Development* **12(3)**: 277–296.

Delft-Hydraulics (1992) *Sudan Flood Early Warning System*. Technical report prepared for the Ministry of Irrigation and Water Resources, Khartoum, Sudan.

Easton ZM, Fuka DR, White ED *et al.* (2010) A multi basin SWAT model analysis of runoff and sedimentation in the Blue Nile, Ethiopia. *Hydrology and Earth System Sciences* **14(10)**: 1827–1841.

Elagib NA and Mansell MG (2000) Recent trends and anomalies in mean seasonal and annual temperatures over Sudan. *Journal of Arid Environments* **45(3)**: 263–288.

Gamachu D (1977) *Aspects of Climate and Water Budget in Ethiopia*. Addis Ababa University, Ethiopia, Library of Congress, open library OL4398638M.

Gaudie AS (2005) The drainage of Africa since the Cretaceous. *Geomorphology* **67(3–4)**: 437–456. See http://www.sciencedirect.com/science/article/pii/S0169555X04002946 (accessed 27/11/2013).

Gismalla YA (1993) *Bathymetric Survey of Roseires Reservoir*. Ministry of Irrigation and Water Resources, The Hydraulics Research Station, Wad Medani, Sudan.

Hamid SH (2001) Sedimentation in Sudanese irrigation systems. *Proceedings of Sediment Transport and Watershed Management Workshop, Khartoum, Sudan* pp. 87–97.

Hassaballah K, Jonoski A, Popescu I and Solomatine DP (2011) Model-based optimization of downstream impact during filling of a new reservoir: case study of Mandaya/Roseires Reservoirs on the Blue Nile River. *Water Resource Management* **26(2)**: 273–293.

HRS (Hydraulics Research Station) (2008) *The Sedimentation in-front of Bait Al mal Pumping Site, Causes and Mitigation Measures*. Ministry of Irrigation and Water Resources, The Hydraulics Research Station, Wad Medani, Sudan.

Hurst HE (1950) *The Nile Basin Volume IIIV; The Hydrology of the Sobat and the White Nile and the Topography of the Blue Nile and Atbara*. Government Press, Cairo, Eygpt, Paper 55.

Hydrosult Inc, Tecsult DHV, Nile Consult, Comatex Nilotica and T&H Consulting (2007) Cooperative Regional Assessment (CRA) for Watershed Management-Trans-Boundary Analysis: Abbay-Blue Nile Sub-Basin, Report to Eastern Nile Technical Regional Office CENTRO:16.

Johnson PA and Curtis D (1994) Water balance of the Blue Nile Basin in Ethiopia. *Journal of Irrigation and Drainage Engineering* **120(3)**: 573–590.

Julien P, Klaassen G, Ten Brinke W and Wilbers A (2002) Case study: bed resistance of Rhine River during 1998 flood. *Journal of Hydraulic Engineering* **128(12)**: 1042–1050.

Kemink E, Wang ZB, de Vriend HJ and van Beek E (2003) Modelling of flood defence measures in the lower Yellow River using SOBEK. *Proceeding of 1st International Yellow River Forum (IYRF) on River Basin Management, Zhengzhou, China*.

Kim U and Kaluarachchi J (2008) Application of parameter estimation and regionalization methodologies to ungauged basins of the upper Blue Nile River Basin, Ethiopia. *Journal of Hydrology* **362(1–2)**: 29–56.

McCartney M, Shiferaw A and Seleshi Y (2009) Estimating environmental flow requirements downstream of the Chara Chara weir on the Blue Nile River. *Hydrological Processes* **23(26)**: 3751–3758.

McGahey C, Knight D, Samuels P and Neill C (2012) Discussion: Advice methods and tools for estimating channel roughness. *Proceedings of the Institution of Civil Engineers – Water Management* **165(7)**: 403–404.

Mohamed YA, van den Hurk BJJM, Savenije HHG and Bastiaanssen WGM (2005) Hydro-climatology of the Nile: results from a regional climate model. *Hydrology and Earth System Sciences* **9(3)**: 263–278.

Naqshband S, Ribberink JS and Hulscher SJMH (2012) Free surface effect on dune morphology and evolution. *Proceeding of NCR-days 2012, Book of Abstracts, Arnhem, the Netherlands*, pp. 45–46.

Nash JE and Sutcliffe JV (1970) River flow forecasting through conceptual models part I – A discussion of principles. *Journal of Hydrology* **10(3)**: 282–290.

Nile Basin Initiative (2003) *Nile Transboundary Environmental Action Project. Project Appraisal Document. Report 24609*. See http://documents.worldbank.org/curated/en/2003/03/2183592/nile-basin-initiative-nile-transboundary-environmental-action-project (accessed 11/04/2003).

Nile Basin Initiative (2004) *Efficient Water Use for Agricultural Production. Report 28266*. See http://documents.worldbank.org/curated/en/2005/02/5643116/africa-region-nile-basin-initiative-efficient-water-use-agricultural-production-project (accessed 16/02/2005).

Paarlberg AJ, Dohmen-Janssen CM, Hulscher SJMH and Termes P (2007) A parameterization of flow separation over subaqueous dunes. *Water Resources Research* **43(11)**: W12417.

Paarlberg AJ, Dohmen-Janssen CM, Hulscher SJMH, Termes P and Schielen R (2010) Modelling the effect of time-dependent river dune evolution on bed roughness and stage. *Earth Surface Processes and Landforms* **35(15)**: 1854–1866.

Prinsen GF and Becker BPJ (2011) Application of SOBEK hydraulic surface water models in the Netherlands Hydrological Modelling Instrument. *Irrigation and Drainage* **60(1)**: 35–41.

Santhi CJ and Arnold G (2001) Validation of the SWAT model on a large river basin with point and nonpoint sources. *Journal American Water Resources Association* **37(5)**: 1169–1188.

Shahin M (1985) *Hydrology of the Nile Basin*, vol. 21. Elsevier, Amsterdam, the Netherlands.

Singh J, Knapp HV and Demissie M (2004) Hydrologic modeling of the Iroquois River watershed using HSPP and SWAT. ISWS CR 2004-08. Champaign, IL: Illinois state water survey.

Smith JD and McLean SR (1977) Boundary layer adjustments to bottom topography and suspended sediment. *Proceeding of the 8th International Liege Colloqium on Ocean Dynamics. Elsevier Oceanography Series* **19**: 123–151.

Sutcliffe JV and Parks YP (1999) *The Hydrology of the Nile*. International Association of Hydrological Sciences (IAHS), The International Water Management Institute, Colombo, Sri Lanka and Gibb Water, Reading, UK, Specific Publication No. 5.

The Dam Speech (2011) *Speech made by P. M. Meles Zenawi of Ethiopia at the Official Commencement of the Renaissance Dam, Grand Millennium Dam*. See http://grandmillenniumdam.net/the-dam-speech/ (accessed 26/04/2011).

Tiesler R (2009) *Roseires Dam Heightening Construction Surveys*. Monaro Surveying Services, Canberra area, Australia, pp. 1–15.

UNESCO (2004) *National Water Development Report for Ethiopia*. Ministry of Water Resources, Addis Ababa, Ethiopia, UN-WATER /WWAP/2006/7, World Water Assessment Report.

US BoR (United States Bureau of Reclamation) (1964) *Land and Water Resources of the Blue Nile Basin. Main Report and Appendices I–V.* Government Printing Office, Washington, DC, USA.

van Liew MW, Arnold JG, Garbrecht JD (2003) Hydrologic simulation on agricultural watersheds: choosing between two models. *Transactions of the American Society of Agricultural Engineers* **46(6)**: 1539–1551.

Vazquez-Amábile GG and Engel BA (2005) Use of SWAT to compute groundwater table depth and stream flow in the Muscatatuck River watershed. *Transactions of the American Society of Agricultural Engineers* **48(3)**: 991–1003.

Wang ZB, Schwaneberg D, Sheofeng Z, Lei G and Marchand M (2007) A one-dimensional-two-dimensional integrated hydraulic model for the Yellow River Delta. In Shang Hongqi & Luc Xiangxin (Eds.). *Proceedings for the 3rd International Yellow River Forum on sustainable water resources management and delta ecosystem maintenance, Dongying, China*. Zhengzhou: Yellow River Conservancy Press: 57–64.

Waterbury J (1979) *Hydropolitics of the Nile Valley.* Syracuse University Press, New York, NY, USA.

Wilbers AWE and Ten Brinke WBM (2003) The response of subaqueous dunes to floods in sand and gravel bed reaches of the Dutch Rhine. *Sedimentology* **50(6)**: 1013–1034.

Williams MAJ and Talbot MR (2009) Late quaternary environments in the Nile Basin. In *The Nile. Origin, Environments, Limnology and Human Use* (Dumont HJ (ed.)). *Monographiae Biologicae* **89**: 61–72. Springer, Netherlands.

Yates D and Strzepek K (1998a) An assessment of integrated climate changes impacts of the agricultural economy of Egypt. *Climate Change* **38(3)**: 261–287.

Yates D and Strzepek K (1998b) Modeling the Nile Basin under climate change. *Journal of Hydrologic Engineering* **3(2)**: 98–108.